Understanding the effect of allosteric regulation of Aurora kinases on inhibitor binding

A thesis submitted to the Graduate School of the University of Minnesota

By

Apoorva Limaye

In partial fulfillment of the requirements for the degree of Master of Science

Adviser: Dr. Nicholas Levinson

May 2021

Acknowledgement

I want to thank my adviser, Dr. Nicholas Levinson, for being an incredibly supportive and motivating mentor. I'd like to thank present and former members of the Levinson laboratory for their help and encouragement. I would also like to thank Dr. Wendy Gordon and Dr. Hai Dang Nguyen for agreeing to be on my thesis committee. Lastly, I'd like to thank my friends and family for all the love and support.

Table of contents

List of figures

Chapter 2: Results and discussions

Chapter 3: Materials and methods

Abbreviations

AurA: Aurora Kinase A

AurB: Aurora Kinase B

AurC: Aurora Kinase C

TACC: transforming acidic coiled-coil protein

PLK1: polo-like kinase 1

CPC: Chromosomal Passenger Complex

INCENP: Inner centromere protein

HM: hydrophobic motif

FRET: Förster resonance energy transfer

Unphos: Unphosphorylated

Phos: Phosphorylated

WT AurA: Wild-type AurA

Introduction:

The Aurora kinase family comprises three serine/threonine protein kinases in mammals: Aurora A (AurA), Aurora B (AurB), and Aurora C (AurC)[1]. AurA and AurB are key elements of a complex signaling network that regulates cell cycle progression through mitosis and cytokinesis[1]. During the late G2 phase, AurA localizes at the centrosome and phosphorylates the transforming acidic coiled-coil protein (TACC), which triggers a cascade of reactions responsible for centrosome maturation and generation of microtubules[2]. The centrosomal pool of AurA also serves as one of the G2/M transition regulators by phosphorylating polo-like kinase 1 (PLK1)[3]. Later in the M phase, another pool of AurA is observed near the spindle microtubules where, along with its partner protein Tpx2, it assists in spindle assembly[4]. AurB forms the chromosomal passenger complex (CPC) with three non-enzymatic partners: Inner centromere protein (INCENP), which activates AurB, and Survivin and Borealin, which aid in anchoring the CPC at various cellular locations from prophase to cytokinesis[2,5]. Early in mitosis, it localizes near centromeres, where it plays an important role in centromeric cohesion and attachment of spindle microtubules at kinetochores[2,6]. The CPC also regulates spindle checkpoint via interactions with multiple checkpoint proteins such as BUBR1, BUB1, and Ndc80[7]. Later in mitosis, the CPC moves to the spindle midzone to stabilize the bipolar spindle assembly[6]. It finally moves to the cleavage furrow during cytokinesis, where it aids in spindle disassembly by interacting with kinesin superfamily proteins[6]. AurC, the third member of the Aurora family, is mainly expressed in germ cells where it acts as a catalytic unit of the CPC during meiosis[8].

As AurA and AurB play a central role in orchestrating various mitotic processes, their overexpression results in mitotic dysregulation associated with tumorigenesis[9,10]. In addition, AurA and AurB form complexes with N-myc and C-myc, stabilizing these oncogenic transcription factors[11,12]. These observations make Aurora kinases attractive targets for cancer therapy. Several small-molecule

inhibitors for Aurora kinases have been developed over the years, of which many are in various stages of clinical trials[13]. As the active site of kinases is highly conserved, it is challenging to develop ATP-competitive inhibitors with high specificity for the target kinase. Kinases belonging to the same family have a high sequence homology making it even more difficult to develop inhibitors that are more selective for one member of the family over the other[14]. These problems were encountered during the development and clinical trials of various aurora inhibitors as well[15,16]. Understanding the allosteric regulation of the aurora kinases would help in identifying differences in protein dynamics that would allow for these closely related kinases to be differentiated by conformational-selective inhibitors.

Like other kinases, the kinase domain of Aurora kinases consists of an N-terminal lobe (N-lobe) and a C-terminal lobe (C-lobe), with the active site situated in the cleft between the two lobes[17]. The N-lobe has five β strands, an αC helix, and an αB helix that connects the β-sheet to the αC helix, forming a shallow pocket (PIF pocket) on the surface of the N-lobe adjacent to the αC helix[18]. The C-lobe is mostly helical and contains a highly dynamic activation loop with a conserved Asp-Phe-Gly (DFG) motif[18]. The αC helix and the activation loop are important regulatory features of kinases[19]. When the kinase assumes an active conformation, the DFG aspartic acid is oriented into the active site to help coordinate Mg-ATP, and the activation loop is extended to allow substrate binding across its surface[20]. This active conformation is also called the DFG-in conformation. In the inactive DFG-out conformation, the aspartic acid is oriented away from the active site and the activation loop is oriented in a manner that blocks substrate binding[20]. The kinases switch between these two key conformations along with various intermediate conformations. The active conformation of most protein kinases is also characterized by the formation of a regulatory spine[21]. The regulatory spine refers to a particular arrangement of conserved hydrophobic residues that play an important role in connecting different parts of the kinase and coordinating their motions[21,22]. In aurora kinases, the hydrophobic spine residue of the αC helix is replaced by a polar glutamine residue that forms hydrogen bonds

with water molecules, forming a water-mediated network between the DFG motif, αC helix, and Glu-Lys salt bridge[23]. Unlike closely related AGC kinases and polo-like kinases, aurora kinases lack the C-terminal hydrophobic motif (HM) that binds to the PIF pocket[23]. Activation of AGC-family kinases requires both activation loop phosphorylation and binding of the HM to the PIF pocket[24]. However, in AurA, the water network aids in allosteric activation of the kinase when Tpx2 binds to the PIF pocket, allowing activation independently of autophosphorylation on the activation loop[23]. This allows AurA to have two separate activation mechanisms: Autophosphorylation of T288 on the activation loop, as seen in the centrosomal pool, and binding of Tpx2 to the PIF pocket, as seen in the spindle pool[18,23].

Along with the autoinhibited DFG-out conformation, AurA also assumes an autoinhibited DFG-in conformation, and phosphorylation of T288 and binding of Tpx2 activate AurA via different mechanisms[25]. Phosphorylated AurA assumes both DFG-in and DFG-out conformations[25]. However, there is a shift from an autoinhibited DFG-in state to an active DFG-in state upon phosphorylation so that the DFG-in subpopulation becomes catalytically active[25]. In contrast, when Tpx2 binds to AurA, it causes a shift from the DFG-out to the DFG-in state[25]. When phosphorylated at T288 and bound to Tpx2 simultaneously, the kinase assumes a very rigid fully active DFG-in conformation[26]. Such doubly-active AurA is observed along the mitotic spindles of melanoma cells lacking the AurA-specific phosphatase PP6[27].

It has been observed that some competitive aurora kinase inhibitors prefer to bind to a particular conformation of the protein[28,29,30]. These inhibitors also induce conformational changes upon binding to the kinase[31]. Such inhibitor-induced conformational changes depend on the intrinsic conformational properties of the kinase[26]. When binding to AurA, the inhibitors can display either positive or negative binding cooperativity with Tpx2 depending on the direction in which they modulate the DFG equilibrium. Studying the effect of the change in DFG equilibrium on preferred binding conformation and binding cooperativity can aid in

better understanding inhibitor selectivity. As the activation loop dynamics are governed in part by autophosphorylation, I decided to examine the binding cooperativity of inhibitors bound to dephosphorylated AurA and compare it with the binding cooperativity trend observed previously by Lake et. al. for phosphorylated AurA in complex with Tpx2.

Many competitive inhibitors of Aurora kinases show selectivity for either AurA or AurB, despite the two kinases having nearly identical active sites[32,33]. This inhibitor selectivity is driven in part by conformational changes induced by allosteric partner-protein interactions[34]. As INCENP activates AurB in a manner similar to Tpx2[35], I wanted to understand how INCENP binding changes the dynamics of AurB compared to the AurA-Tpx2 interaction. It has been observed that changing a single amino acid residue at position 198 of AurA from Gly to Asn results in a mutant that preferentially binds to INCENP over Tpx2 and localizes with the CPC instead of polar or spindle pools of AurA[36]. I used G198N AurA to study the effects of INCENP binding on the conformation of the kinase and how it affects inhibitor cooperativity. Since the active sites of AurA and G198N AurA are identical, investigating the effects of INCENP binding on the conformational dynamics of G198N AurA will shed light on the role of allosteric activator proteins in tuning the kinase-drug interaction profile.

Results and discussion:

Activation loop phosphorylation modulates binding cooperativity by affecting AurA-Tpx2 interaction

Catalytically active and inactive states of AurA bound to kinase inhibitors have been observed in abundant X-ray structures[32,37,38]. Based on these x-ray structures, the inhibitors are grouped into two classes. Type I inhibitors bind to the DFG-in state or have no conformational preference, and Type II inhibitors bind to the inactive DFG-out state[26]. As static x-ray structures provide little insight into the dynamic behavior of kinases, spectroscopic tools can be used to elucidate the transition of the kinase between active and inactive states and the effects of allosteric modulators and inhibitors on these states.

Lake et. al. used time-resolved Förster resonance energy transfer (FRET) to dissect the effects of phosphorylation and Tpx2 binding on the conformational properties of AurA[26]. They studied the conformational dynamics of four distinct states of AurA: Phosphorylated on T288 (Phos) on the activation loop, Dephosphorylated (Unphos), Phos+Tpx2, and Unphos+Tpx2[26]. Their assay confirmed that the activation loop phosphorylation results in a shift from autoinhibited DFG-in state to active DFG-in state, and Tpx2 binding causes a shift from the DFG-out to DFG-in state[26].

Lake et. al. then studied the effects of 24 kinase inhibitors on each of the four biochemical states of AurA[26]. Based on the inhibitor-induced conformational changes, they classified these inhibitors into three categories: Type I inhibitors that promote the DFG-in state, Type I inhibitors that promote the DFG-out state, and Type II inhibitors[26]. Lake et. al. also tested how Tpx2 affects the binding affinities of these inhibitors. They observed that conformational preferences of inhibitors dictate the binding selectivity for a specific activation state of AurA[26]. When bound to phos AurA+Tpx2, Inhibitors with a strong preference for the DFG-in state

induced a shift in the DFG equilibrium in the same direction as that of Tpx2, resulting in positive binding cooperativity with Tpx2[26]. On the other hand, the negatively cooperative inhibitors were those that favored the DFG-out state and caused a shift in the DFG equilibrium in an opposite direction as that of Tpx2[26].

Activation loop phosphorylation can have an impact on the cooperativity of inhibitors as it affects Tpx2 binding and alters the DFG-in state[25]. As Lake et. al.'s cooperativity study focused on phos AurA+Tpx2, I decided to determine the binding cooperativity for the same set of inhibitors bound to unphosphorylated AurA+Tpx2 and compare it with Lake et. al.'s phos AurA+Tpx2 data to understand the effect of activation loop phosphorylation on inhibitor-induced conformational changes and cooperativity.

I used a FRET sensor to track the movement of the activation loop of AurA. The sensor was constructed by incorporating cysteine residues to attach two fluorescent dyes on the relatively static D-helix and the dynamic activation loop, with high FRET corresponding to the DFG-out state and low FRET with the DFG-in state (Figure 1A). Binding curves for all 24 inhibitors were obtained in the presence of increasing concentrations of Tpx2 by collecting steady-state FRET data using the Spectral Unmixing Plate Reader[39], an instrument that records the full fluorescence emission spectrum on a well-by-well basis, and then fitting the reference spectra for the donor, the acceptor, and the water Raman peak, to determine spectrally unmixed acceptor to donor ratios.

The cooperativity between the inhibitors and Tpx2 was determined by globally fitting the binding data for inhibitors to a two-state thermodynamic model (Figure 1C) using the numerical simulation program KinTek Explorer. The binding affinity of an inhibitor is altered by the allosteric interaction between Tpx2 and AurA. At the same time, inhibitor binding also affects the binding affinity of Tpx2. When opposing conformational changes are induced by the inhibitor and Tpx2, the binding affinity of one ligand may decrease in the presence of a saturating

concentration of the other ligand, and the opposite can be true when the conformational change induced by the two is similar. In the two-state model (Figure 1B), this binding cooperativity is described in terms of the cooperativity factor α. Because it's a closed thermodynamic cycle, α represents the fold change in Tpx2 affinity in the presence of saturating inhibitor as well as the fold change in the inhibitor affinity in the presence of saturating Tpx2. α values smaller than 1 indicate positive cooperativity and α values greater than 1 indicate negative cooperativity.

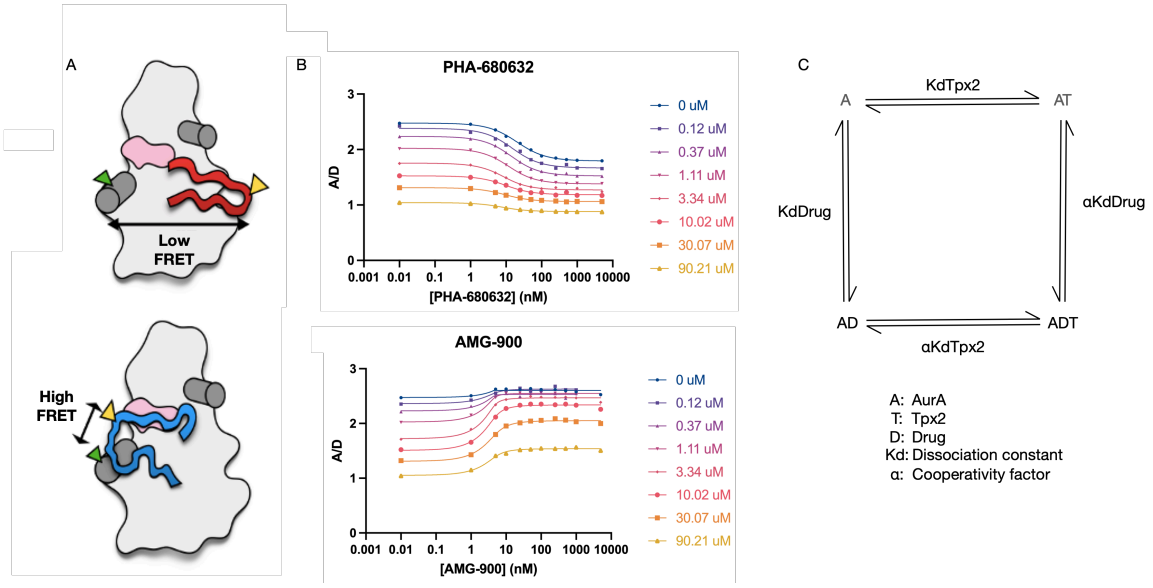

Figure 1: **Determination of binding cooperativity. A)** labeling scheme showing the positions of the two dyes on the αD helix and the activation loop in the inactive DFG-out (blue) and the active DFG-in (red) states. **B)** Fluorescence binding data for a DFG-out inducer (left) and a DFG-in inducer (right). The ratio of the acceptor and donor intensities quantified from emission spectra is plotted against inhibitor concentration. The graph shows two simultaneous titrations, the vertical one for Tpx2 and the horizontal one for the inhibitor. As the concentration of Tpx2 increases, the DFG equilibrium is moved towards the active DFG-in state, as seen by a decrease in the A/D fluorescence intensity ratio. Negatively cooperative inhibitors like AMG-900 shift the DFG equilibrium in an opposite direction towards the DFG-out state. This can be seen by an increase in the A/D ratio observed with increasing inhibitor concentration. The opposite is seen with positively cooperative inhibitors, such as PHA-680632, where both Tpx2 and the inhibitor shift the DFG equilibrium towards the DFG-in state **C)** the two-state thermodynamic model used to determine the cooperativity factor α for the inhibitors.

A cooperativity trend was obtained by arranging the α values of the inhibitors in ascending order. I compared this cooperativity trend to the one observed in the

phos AurA+Tpx2 study to understand the effects of activation loop phosphorylation on inhibitor binding. The inhibitors in the phos AurA+Tpx2 study were separated into two groups: positively cooperative DFG-in inducers and negatively cooperative DFG-out inducers, with the exception of SNS-314. Although I observed a similar cooperativity trend for unphos AurA for most inhibitors, Hesperadin, TAE-684, and TAK-901 showed positive binding cooperativity in this study based on their α values, rather than the negative cooperativity observed with phos AurA (Figure 2B).

Most type I inhibitors that were shown to induce a DFG-in shift in the phos AurA study remained positively cooperative with α values less than 1. SNS-314 continued to be negatively cooperative despite being a DFG-in inducer[40]. This is because SNS-314 can reach into the back of the active site and interact with the DFG-motif and the αC helix[40], resulting in the αC helix being pushed outwards, weakening the binding of Tpx2[26].

Type I inhibitors like PHA-680632, CCT-137690, and CCT-129202 show greater positive cooperativity with unphos AurA than phos AurA. Ruff et. al. showed that the activation loop of unphos AurA, even when bound to Tpx2, is more dynamic than the activation loop of phos AurA[31] The less constrained activation loop of unphos AurA may orient in a way to assume a DFG-in conformation that favors binding of both Tpx2 and these inhibitors resulting in greater positive cooperativity than that observed with phos AurA+Tpx2.

ENMD-2076, a type I AurA inhibitor, shows reduced positive cooperativity. ENMD-2076 preferentially recognizes the active DFG-in substate promoted by activation loop phosphorylation[26]. As this substate is absent in the case of unphos AurA, the binding affinity of the inhibitor is reduced. Lake et. al. showed that inhibitors induce a DFG-in shift by interacting with a pocket under the P loop of the kinase[26]. They also showed that JNJ-7706621 only interacts with the valine side chain near the active site and doesn't extend into the P-loop pocket[26]. I observed that Tpx2 binds

weakly to unphos AurA resulting in a smaller DFG-in shift induced by Tpx2 binding. The small conformational change induced by JNJ-7706621 along with a smaller shift in DFG equilibrium for unphos AurA+Tpx2 explains the higher α value for this inhibitor when bound to the unphos+Tpx2 complex.

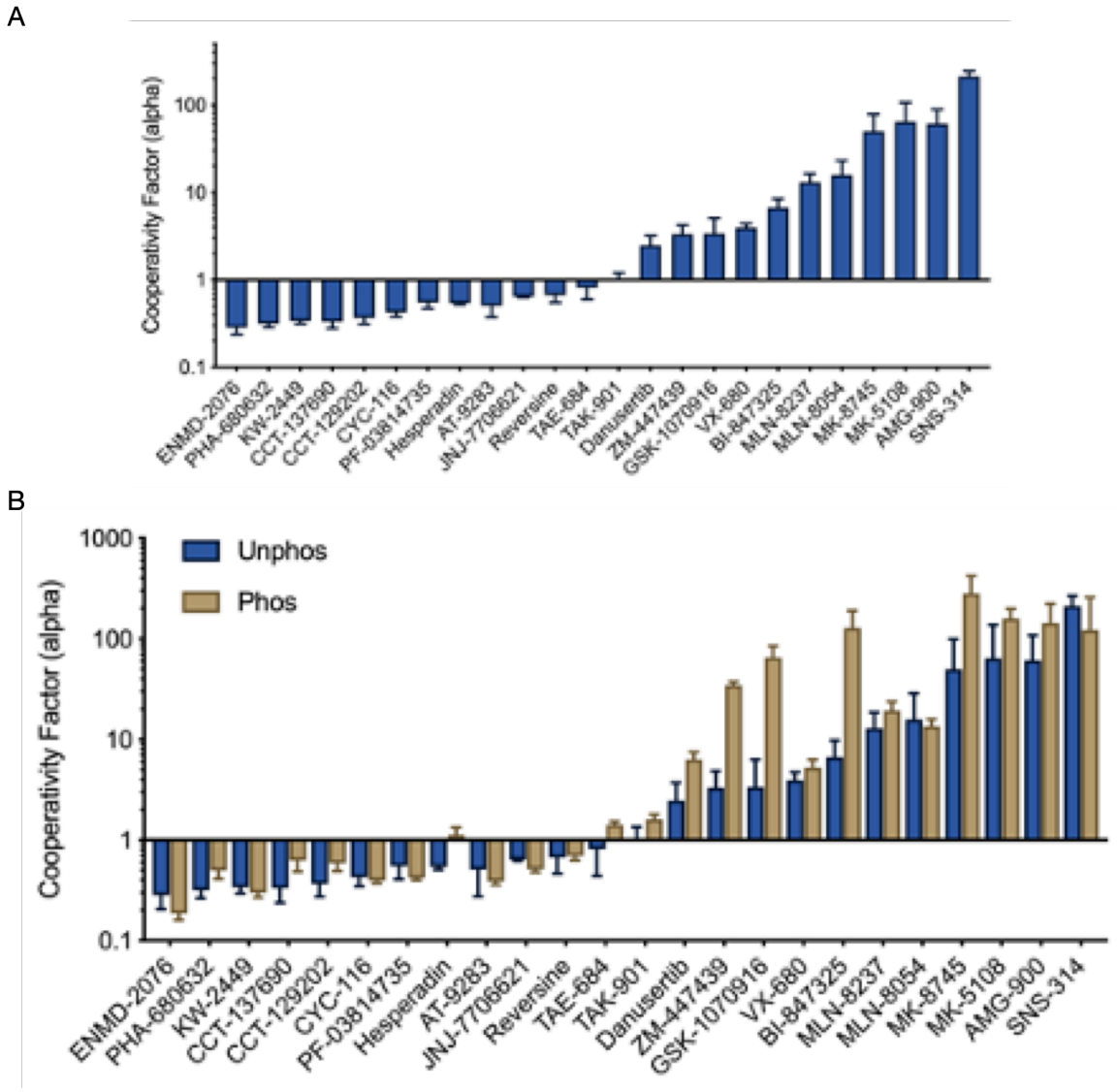

Figure 2: Comparison of inhibitor binding-cooperativities. A) The DFG-in inducers are positively cooperative with α values less than 1. The DFG-out inducers are negatively cooperative with α values greater than 1. SNS-314 is an exception as it reaches deeper into the binding pocket and pushes the αC-helix outwards, thus hindering Tpx2 binding[26]. **B)** Comparison of binding cooperativity trends of phos and unphos Aurora A with Tpx2.

In the phos AurA study, Danusertib, MLN-8054, MLN-8237, and X-680 cause partial shifts towards the DFG-out state[26]. VX-680 and Danusertib were the weakest DFG-out inducers, followed by the MLN compounds[26]. It was reported in the phos AurA study that inhibitors that trigger a full conformational shift to the DFG-out state have α values between 35 to 300, indicating strong negative cooperativity. For inhibitors that caused a partial shift towards the DFG-out state that can be overridden by Tpx2 binding, the α values were less than 30, indicating weaker negative cooperativity[26]. The results for unphos AurA+Tpx2 are similar to the phos AurA+Tpx2 findings with AMG-900, MK-5108, and MK-8745 showing strong negative cooperativity with α values greater than 35 and Danusertib, MLN-8054, MLN-8237, and VX-680 showing weak negative cooperativity with α values between 1 to 30.

The difference in binding cooperativity when bound to unphos vs phos AurA was more pronounced for AurB inhibitors such as BI-847325, ZM-447439, and GSK-1070916. For unphos AurA, I observed that the α values for these compounds were less than 10, indicating that they show weak negative cooperativity with unphos AurA+Tpx2. The reported α values for these AurB inhibitors bound to phos AurA+Tpx2 were in a range of 35 (ZM-447439) to 128 (BI-847325). The reduced negative cooperativity suggests that the less constrained unphos AurA+Tpx2 complex permits the AurB inhibitors to bind to their preferred conformation with relatively little resistance compared to the phos AurA+Tpx2 complex.

Discussion

The regulatory spine residue on the αC helix of AurA is a polar Gln residue that facilitates the formation of a water-mediated network between the αC helix, DFG motif, and Glu-Lys salt bridge[23]. This allows AurA to have two independent modes of activation[23]. When Tpx2 binds to AurA, it activates the kinase by stabilizing the water network and inducing a shift from autoinhibited DFG-out state to active DFG-in state[23]. Phosphorylation on its own does not induce a shift from DFG-out to

DFG-in equilibrium, but it induces a shift from autoinhibited DFG-in substate to active DFG-in substate[25]. Both unphos and phos AurA sample between the DFG-out and DFG-in state, but phosphorylation stabilizes the substrate-binding segment of the activation loop and locks the kinase in a single DFG-in conformation via ionic interactions between the phosphothreonine and three arginine residues[25]. These ionic interactions are absent in unphos AurA. The activation loop of unphos AurA is highly dynamic compared to the activation loop of phos AurA[25]. Orientation of the activation loop into an active DFG-in substate results in formation of the Tpx2 interaction surface by the N-terminal segment of the activation loop, enhancing the binding affinity of Tpx2 to phos AurA[25]. Tpx2 binds tightly to phos AurA and further stabilizes the active DFG-in state[25]. MD simulations have shown that the activation loop of unphos AurA bound to Tpx2 remains more dynamic than phos AurA[25]. Tpx2 also binds more weakly to unphos AurA. This results in unphos AurA+Tpx2 complex being less constrained than phos AurA+Tpx2. The inhibitors that preferred binding to a slightly different DFG-in state than the active DFG-in substate showed higher positive cooperativity in this unphos AurA study, as the less constrained unphos AurA could probably assume a DFG-in conformation that facilitated binding of both the inhibitor and Tpx2. For most DFG-out inducers, the less constrained nature of the unphos AurA+Tpx2 complex resulted in slightly dampened binding cooperativity compared to phos AurA+Tpx2. However, the binding cooperativity data for AurB inhibitors bound to unphos vs phos AurA+Tpx2 were quite different. The α values for AurB inhibitors bound to phos AurA+Tpx2 indicated very strong negative cooperativity. As unphos AurA was probably more accommodating of the conformational preferences of these AurB inhibitors, there was a drastic reduction of the α values of all AurB inhibitors when bound to unphos AurA. Inhibitor-induced conformational changes depend on the intrinsic conformational equilibrium of the kinase. This suggests that the greater flexibility of unphos AurA facilitates binding of AurB and pan aurora inhibitors to their preferred DFG conformations.

AurB inhibitors are positively cooperative with unphosphorylated INCENP bound to G198N AurA

The kinase domains of AurA and AurB have 70% sequence homology, yet their cellular localization and functions are completely different[41]. Activity of the CPC is tightly regulated by its non-enzymatic subunits, especially INCENP[42]. The C-terminal region of INCENP binds to the N-lobe of AurB and partially activates the kinase[43]. The partially activated AurB phosphorylates the threonine residue at position 232 on the activation loop as well as the two serines of the conserved TSS motif of INCENP[43]. In addition, the checkpoint kinase 1 (chk1) phosphorylates a serine residue at position 311 on the C-lobe of AurB in vivo, resulting in a fully active AurB-INCENP complex[44]. I was interested in understanding the effects of INCENP binding on the dynamics of AurB, which in turn would influence binding affinity, conformational preference, and cooperativity of inhibitors.

For the preliminary experiments, I decided to use a mutant of AurA obtained by changing a single amino acid at position 198 from Gly to Asn. The G198N AurA behaves like AurB in cells and can complement AurB knockdown[36], as it preferentially binds to the AurB activator INCENP over Tpx2 and localizes with the CPC instead of polar or spindle pools of AurA[36]. The mutant also binds to AurB substrates, implying a change in its cellular activities[36]. These findings emphasize the effect of allosteric interactions on the structure and in turn function of a protein. The active sites of AurA and AurB differ by three amino acids, of which Thr217 of AurA plays an important role in binding of certain inhibitors such as MLN8054[41]. The active site of G198N AurA is identical to that of WT AurA, so any changes observed in the binding patterns of the inhibitors would be solely due to conformational changes induced by the allosteric interaction with the partner-protein INCENP.

I determined the binding affinity of INCENP for G198N AurA using steady-state FRET. I expressed the C-terminal portion of human INCENP (823-901) in E. coli

cells and purified the peptide by affinity chromatography. This region of INCENP has been shown to interact with AurB in crystal structures[45]. The G198N AurA FRET sensor was prepared in a similar manner to unphos AurA sensor. Fluorescence emission was recorded for each concentration of INCENP from 0 to 1600 nM titrated against 5 nM kinase.

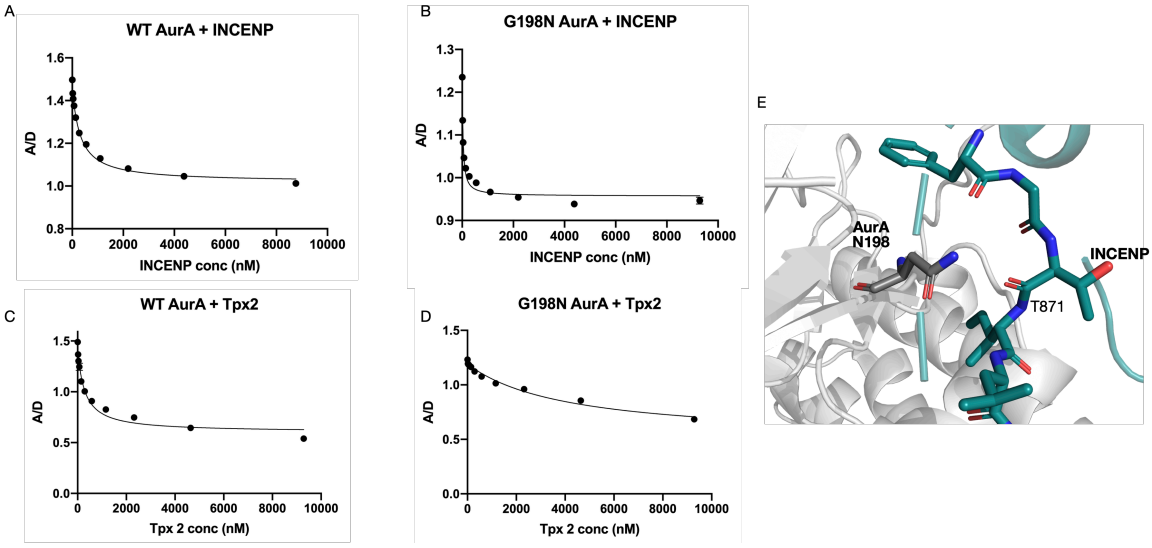

Figure 3: Determination of the binding affinity of INCENP for G198N AurA. Increasing concentrations of Tpx2 and INCENP were titrated against 5 nM WT and mutant Aurora A FRET sensor. The ratio of acceptor to donor intensities quantified from emission spectra is plotted against partner protein concentration. Kd is calculated using quadratic binding equation. **A, B)** INCENP binds tighter to the mutant compared to the WT AurA. **C, D)** Tpx2 binds tighter to WT Aurora A compared to the mutant. **E)** H bond between N198 of AurC (blue, PDB ID 6GR8) and INCENP residue T871 (orange).

Fu et. al. used a mutant of AurB that had the Asn at position 142, an equivalent residue to Gly 198 of AurA, changed to Gly[36]. Through immunoprecipitation, they found that N142G AurB bound less INCENP than WT AurB[36]. They also observed that INCENP binds to WT AurA in vitro, and this interaction was reduced by the addition of Tpx2[36]. I observed that INCENP binds to both WT (Kd = 300 nM) and G198N (Kd = 30 nM) AurA, although its binding affinity for WT AurA is substantially lower than that for G198N AurA.

Crystal structures show that the surface of the N-lobe of AurB/C that is adjacent to the PIF pocket interacts with a small helical region of INCENP[45]. This part of the N-lobe has a highly conserved sequence LRLYXY found in all three mammalian Aurora kinases, where X represents a Gly residue in AurA (G198 in human AurA) and an Asn residue in AurB/C (N142 in human AurB and N108 in human AurC). The Gly and Asn residues are conserved in lower organisms as well. The crystal structure of xenopus AurB shows that the conserved Asn of AurB/C forms hydrogen bonds with Y825 and I828 of xenopus INCENP[36]. I believe that similar interaction can be observed with N198 of mutant AurA with T871 residue of human INCENP (Figure 3E). These interactions are lacking between INCENP and WT AurA due to the absence of the polar Asn on the N-lobe binding surface, which explains the 10-fold higher Kd value of INCENP for WT AurA compared to G198N AurA.

The crystal structure of human AurA with Tpx2 shows two segments of Tpx2 interacting with the PIF pocket and the αC helix of AurA[46]. Residues 7-21 of Tpx2 interact with the PIF pocket and the adjacent surface on the N-lobe of AurA, and residues 30-43 of Tpx2 interact with the αC helix[46]. In the AurA-Tpx2 complex, Gly 198 of AurA is in van der Waals contact with Pro 13 of Tpx2[46]. If this Gly is replaced with an amino acid with a side chain, such as Asn, the side chain hinders Tpx2 binding resulting in weakened affinity. Fu et. al. observed that when Gly 198 was replaced with Ala, Leu, or Val, the mutant kinase localized to the centromere and midzone instead of localizing with the CPC[36]. I observed that Tpx2 binds more strongly to WT AurA (Kd = 284 nM) compared to G198N AurA (Kd = 4085 nM), which underscores that side-chain length and polarity of the residue at position 198 of AurA has a major influence on the binding of Tpx2.

The C-terminal IN-box of INCENP contains a highly conserved TSS motif. In vivo, upon binding to AurB/C, this motif is phosphorylated by AurB/C. INCENP binding also facilitates AurB/C autophosphorylation on the activation loop. Both these phosphorylation processes are important for the formation of a fully active

AurB/C+INCENP complex. Although I've shown that INCENP binds G198N AurA with low nanomolar affinity, I believe that the binding affinity of INCENP will significantly increase when the IN-box TSS motif is phosphorylated[41]. The two serine residues of the TSS motif are conserved through evolution[47]. The IN-box helical region of INCENP is fully engaged with the αC helix and the activation loop of AurB after TSS phosphorylation[47]. INCENP with unphosphorylated TSS motif bound to G198N AurA forms an intermediate complex that's not fully active[48]. I used this complex to determine inhibitor cooperativity for INCENP to understand how the partially active G198N AurA+INCENP complex responds to allosteric inputs.

Inhibitor binding cooperativity was determined using phos G198N AurA FRET sensor. Binding curves for all 24 inhibitors were obtained in the presence of increasing concentrations of INCENP by collecting steady-state FRET data using the Spectral Unmixing Plate Reader[39], and then fitting the reference spectra for the donor, the acceptor, and the water Raman peak, to determine spectrally unmixed acceptor to donor ratios. The ratio of the acceptor and donor intensities quantified from emission spectra was plotted against inhibitor concentration for all 24 inhibitors. The graphs show two simultaneous titrations, the vertical one for INCENP and the horizontal one for the inhibitor. As the concentration of INCENP increases, the DFG equilibrium is moved towards the active DFG-in state, as seen by a decrease in the A/D fluorescence intensity ratio. Negatively cooperative inhibitors shift the DFG equilibrium in the opposite direction towards the DFG-out state. This can be seen by an increase in the A/D ratio observed with increase in the inhibitor concentration. The opposite is seen with positively cooperative inhibitors, where both INCENP and the inhibitor shift the DFG equilibrium towards the DFG-in state. I also plotted the Kd values of inhibitors as a function of the concentration of INCENP to determine the effect of INCENP binding on the binding affinity of the inhibitor.

Kd plots for Type I DFG-in inducers indicate that these inhibitors bind tighter in the presence of INCENP (Figure 4). The graphs of A/D ratio plotted against inhibitor concentration for DFG-in inducers like TAE-684 and PF-03814735 show that the shift induced in the DFG equilibrium by INCENP and the inhibitor is in the same direction and that this is why these inhibitors are positively cooperative with INCENP. Unphos INCENP has been shown to not anchor the activation loop in a rigid DFG-in state[20]. G198N AurA may assume a DFG-in state that facilitates binding of both INCENP and the inhibitor, resulting in improved binding affinity of inhibitors in presence of INCENP.

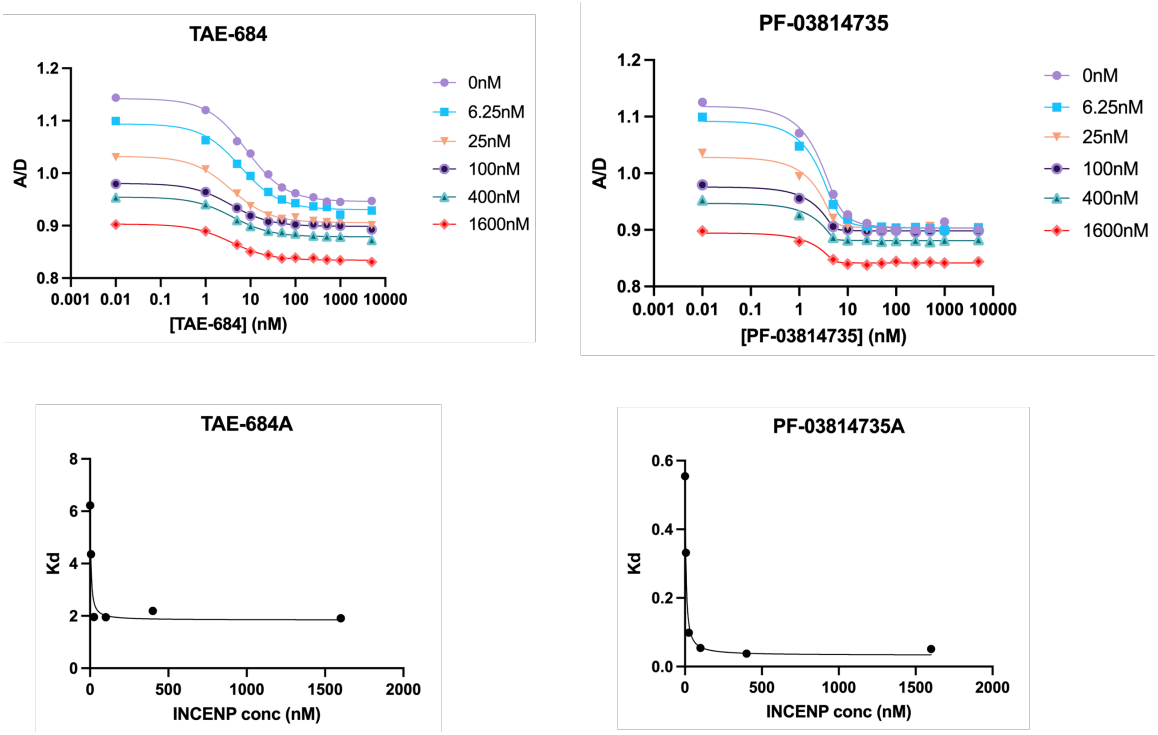

Figure 4: DFG-in inducers TAE-684 and PF-03814735 are positively cooperative with INCENP. Fluorescence binding data for DFG-in inducers TAE-684 and PF-03814735. The ratio of the acceptor and donor intensities quantified from emission spectra is plotted against inhibitor concentration. The graph shows two simultaneous titrations, the vertical one for INCENP and the horizontal one for the inhibitor. As the concentration of INCENP increases, the DFG equilibrium is moved towards the active DFG-in state, as seen by a decrease in the A/D fluorescence intensity ratio. Positively cooperative inhibitors shift the DFG equilibrium in the same direction towards the DFG-in state, as seen by decrease in the A/D ratio observed with increase in the inhibitor concentration. The Kd plots indicate that the inhibitors are binding more tightly in the presence of INCENP.

Varying results were seen for binding cooperativity of partial DFG-out inducers. The MLN compounds showed weakened binding affinity in presence of INCENP as their Kd value increased with increasing INCENP concentration. VX-680, the weakest DFG-out inducer in Lake et. al.'s study binds tighter in the presence of INCENP, indicating positive cooperativity with INCENP (Figure 5). In contrast to what's seen with Tpx2, SNS-314 binds tighter in presence of INCENP (Figure 5). Unphos INCENP does not make extensive interactions with R90, H97, and H190 residues, as Tpx2 does. This may allow SNS-314 to bind the kinase by displacing the αC helix even when INCENP is bound to the kinase. One of the strongest DFG-out inducers, AMG-900, continues to be negatively cooperative with INCENP as its binding gets weaker in presence of INCENP (Figure 5).

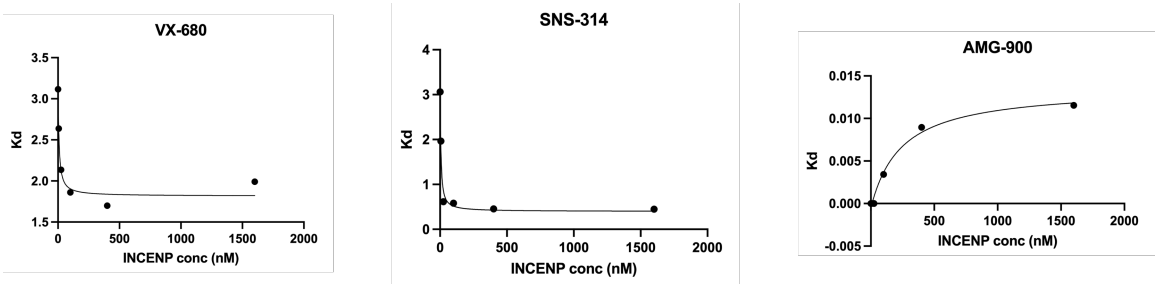

Figure 5: Kd plot for VX-680 and SNS-314 suggest that these inhibitors bind tighter in presence of INCENP, indicating positive cooperativity. Kd plot for AMG-900 (right) shows an increase in Kd value with increasing INCENP concentration, suggesting that the inhibitor is negatively cooperative with and binds weaker in presence of INCENP.

AurB inhibitors, GSK-1070916, Hesperadin, and BI-847325 are positively cooperative with INCENP as seen by a decrease in their Kd values with increasing INCENP concentrations (Figure 6). INCENP wraps around the N-lobe of AurB, increases the separation between the two lobes, and opens the active site by forming extensive contacts with the N-lobe via its αB helix, allowing inhibitors to access the hydrophobic back pocket of the kinase. Inhibitors like Hesperadin and BI-847325 probably access the hydrophobic back pocket and stabilize G198N AurA in the DFG-in state by forming hydrophobic contacts. As a result, Hesperadin, which is non-cooperative when bound to phos WT AurA+Tpx2, and BI-847325, which is negatively cooperative when bound to phos WT AurA+Tpx2, are both

positively cooperative with G198N AurA+INCENP. The change in the Kd values of JNJ-7706821 and ZM-447439 also indicated that the inhibitors bind slightly better in presence of INCENP.

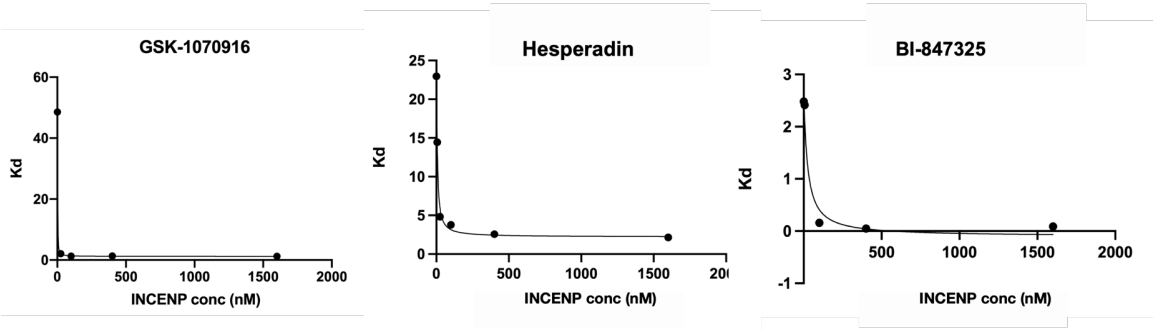

Figure 6: AurB inhibitors are positively cooperative with INCENP and bind tighter in presence of it as seen in the Kd plots.

Discussion

For these preliminary cooperativity assays, I used the same 24 inhibitors that were used for unphos AurA+Tpx2 and Phos AurA+Tpx2 studies. Unlike AurB, the active site of G198N is identical to WT AurA. If inhibitors interact differently when binding to G198N AurA/INCENP compared to WT AurA/Tpx2, it must be due to changes in the allosteric interaction as the binding site encountered by the inhibitors has the exact same amino acid sequence. DFG-in inducers, such as CYC-116, KW-2449, PF-03814735, AT-9283, etc., remained positively cooperative and DFG-out inducers, such as MK-8745 and AMG-900, remained negatively cooperative. Unphos INCENP bound to phos G198N AurA is mimicking a partially active AurB-INCENP complex. This complex would be more flexible than a fully active AurB-INCENP complex due to the lack of extensive interactions between the TSS motif and the activation loop. This would allow the phos G198N AurA+unphos INCENP complex to assume a conformation that is close to the preferred binding conformation of the inhibitors. This could explain why there was no change seen in the cooperativity for most inhibitors bound to G198N AurA+INCENP.

Inhibitors like VX-680, SNS-314, and most AurB inhibitors showed a stark difference in their binding cooperativity with INCENP compared to Tpx2

cooperativity assays. This change could be due to unphos INCENP forming a more extensive contact with the N-lobe, causing the two lobes of the kinase to separate further allowing the inhibitors to access the hydrophobic back pocket, while not locking the αC helix and the activation loop in a very constrained conformation that might interfere with inhibitor binding. The more rigid structure of fully active AurB+INCENP may behave in a more similar manner to phos AurA+Tpx2. The complex will be more stable and constrained, probably resulting in more dramatic inhibitor cooperativity effects based on the conformational preference of inhibitors.

Materials and Methods:

WT Aurora A expression and purification[26]**.** A construct of human Aurora A (residues 122-403 and an N-terminal polyhistidine tag) was cloned into pETM11 vector. Construct was expressed in BL21-DE3-RIL cells. A starter culture was grown overnight at 37°C and 250 rpm. Cells from starter culture were transferred to terrific broth with 0.1% glycerol and grown at 37°C and 250 rpm till OD was 1-1.2. Expression was induced with 1 mM IPTG at 18°C for 18 hours. Cultures were centrifuged to collect cell pellets. Cells were resuspended in lysis buffer (50 mM Tris, pH 8.0, 500 mM NaCl, 10% glycerol, 25 mM imidazole). Cells were lysed using homogenizer, and the lysate was centrifuged using JLA25.5 rotor at 20000 rpm at 4°C for an hour. The supernatant was filtered and loaded onto a HisTrap Ni-NTA column. The protein was eluted using elution buffer (50 mM Tris, pH 8.0, 500 mM NaCl, 10% glycerol, 500 mM imidazole). Buffer exchanged into desalting buffer (50 mM HEPES, pH 7.5, 300 mM NaCl, 10% glycerol) using HiPrep 26/10 desalting column.

Cation exchange chromatography was used to get a homogenous phosphorylation state. Salt concentration of the protein pool was adjusted to match salt concentration of Buffer A (20 mM HEPES, pH 7.2, 50 mM NaCl, 10% glycerol) prior to loading in onto SP HP column. Eluted with fixed volume fractionation with 0 to 40% gradient of buffer B (20 mM HEPES, pH 7.2, 1 M NaCl, 10% glycerol) over 20 column volumes. Eluted protein was divided into two fractions. A fraction of phosphorylated Aurora A was incubated with lambda protein phosphatase and 10mM MnCl2 at 30°C and 60 rpm for an hour. Salt concentration was adjusted, and cation exchange procedure was repeated to get unphosphorylated Aurora A.

G198N Aurora A expression and Purification. site directed mutagenesis was used to replace the Gly at residue 198 of WT human Aurora A to Asn. Same protocol as above was followed for expression and purification.

Preparing the FRET sensor[26]**.** site directed mutagenesis was used to replace solvent exposed Cys at residues 290 and 393 with Ala and Ser respectively. Cysteines were introduced at residue 225 on the D-helix and residue 284 on the activation loop. Alexa fluor 488 C5 maleimide was used as a FRET donor dye. Donor was labelled in a 1:0.9 protein to dye ratio for 2 hours at 4°C. Signally labelled Sample was collected using cation exchange using protocol mentioned earlier. Alexa fluor C5 maleimide 568 was used as a FRET acceptor dye. The sample was incubated with 2x concentration of dye at 4°C for 4 hours. The FRET label was desalted into labelling buffer using HiTrap desalting column.

INCENP expression and purification. A construct of human INCENP (residues 823-899, N terminal GST tag with TEV cleavage site and non-cleavable C-terminal polyhistidine tag) was expressed in BL21-DE3-RIL cells. A starter culture was grown overnight at 37°C and 250 rpm. Cells from starter culture were transferred to terrific broth with 0.1% glycerol and grown at 37°C and 250 rpm till OD was 1.5. Expression was induced with 1 mM IPTG at 18°C for 18 hours. Cultures were centrifuged to collect cell pellets. Cells were resuspended in lysis buffer (8M Urea, 50 mM Tris, pH 8.0, 500 mM NaCl, 5% glycerol, 25 mM imidazole, 1.5mM DTT). Part of the purification was carried out under denaturing conditions. Cells were lysed using homogenizer, and the lysate was centrifuged using JLA25.5 rotor at 20000 rpm at room temperature for 30 minutes. The supernatant was filtered and loaded onto a HisTrap FF crude Ni-NTA column. The protein was eluted using elution buffer (8M Urea, 50 mM Tris, pH 8.0, 500 mM NaCl, 10% glycerol, 500 mM imidazole). Buffer exchanged into desalting buffer (50 mM HEPES, pH 7.5, 300 mM NaCl, 10% glycerol) using HiPrep 26/10 desalting column. Buffer exchanged by overnight dialysis at 4°C into dialysis buffer (50 mM Tris, pH 8.0, 500 mM NaCl, 5% glycerol, 2.5mM DTT). Protein sample was desalted into TEV loading buffer/Ni column lysis buffer (50 mM Tris, pH 8.0, 500 mM NaCl, 10% glycerol, 25 mM imidazole). Incubated at 4°C with TEV protease for 18 hours. Peptide was captured with HisTrap FF Ni-NTA column. Gradient elution with fixed volume fractionation

over 0-100% gradient of elution buffer (50 mM Tris, pH 8.0, 500 mM NaCl, 10% glycerol, 500 mM imidazole).

Tpx2 expression and purification[26]**.** A construct of human Tpx2 (residues 1-43, N-terminal GST tag with prescission protease cleavage site) was expressed in BL21-DE3-RIL cells. A starter culture was grown overnight at 37°C and 250 rpm. Cells from starter culture were transferred to terrific broth with 0.1% glycerol and grown at 37°C and 250 rpm till OD was 1-1.2. Expression was induced with 1 mM IPTG at 18°C for 18 hours. Cultures were centrifuged to collect cell pellets. Cells were resuspended in GST lysis buffer (PBS, pH 7.4, 5% glycerol). Cells were lysed using homogenizer, and the lysate was centrifuged using JLA25.5 rotor at 20000 rpm at 4°C for an hour. Protein was captured using Millipore GST column. Protein was eluted with GST elution buffer (PBS, pH 7.4, 5% glycerol, 20 mM reduced glutathione). Sample was incubated with prescission protease overnight at 4°C. Peptide was separated from the rest of the sample by gel filtration using Superdex 16/600 column. Gel filtration sample was injected on HPLC and gradient elution was performed with HPLC buffer A (Milli-Q water and 0.1% TFA) and Buffer B (acetonitrile and 0.1% TFA). Eluate was lyophilized and reconstituted in Tpx2 buffer (0.25mM Tris-HCl, PH 7.5)

FRET assay to determine binding cooperativity[26]**.** 24 commercially available Aurora kinase inhibitors were used for the FRET assay. Prepared ten different concentrations of the inhibitors for the assay by making serial dilutions to get 50x stock solutions of 0.05, 0.25, 0.5, 1.25, 2.5, 5, 12.5, 25, 50, and 500 μM concentrations in DMSO. Master drug plates were prepared by transferring these stock solutions into 96-well plates. 1μL stock solutions were transferred to 384-well plate so that the final concentrations after adding FRET sensor and partner-protein samples would be 1, 5, 10, 25, 50, 100, 250, 500, 1000, 5000 nM. Wells on all four edges of the 384-well plate contained control DMSO solutions. Inhibitors were titrated as per the layout below. 5nM FRET sensor and serial dilutions of partner protein in ADP quest buffer (15 mM HEPES, pH 7.4, 20 mM NaCl, 1 mM

EGTA, 0.02% Tween-20, 10 mM MgCl2, 0.5 mg/mL BGG, 1% DMSO) were added to each row of the inhibitors. The plates were incubated at room temperature for 90 minutes, then shaken for 10 seconds, and centrifuged for a minute at 100 g. Steady state fluorescence data was collected using Spectral Unmixing Plate Reader (SUPR). Donor and acceptor contribution to fluorescence emission was calculated by fitting the reference spectrum of each fluorophore and removing the Raman effect contributed by the solvent. Two-site binding cooperativity model was used to analyze the data.

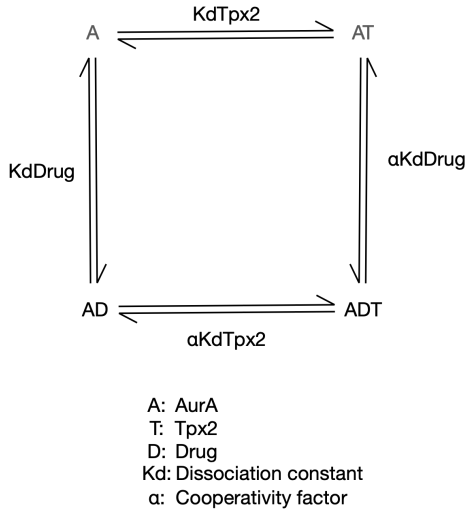

Figure 7: The two-state binding cooperativity model.

In this model, A is Apo AurA, AD is AurA and drug complex, AT is AurA and Tpx2 complex, and ADT is a ternary complex comprising of AurA, Tpx2, and the drug. Kd Drug is and Kd Tpx2 are equilibrium dissociation constants for drug and Tpx2 binding to Apo AurA. α represents the fold change in Tpx2 affinity in presence of saturating inhibitor as well as the fold change in the inhibitor affinity in presence of saturating Tpx2. The value of α must be the same for drug and Tpx2 as it's a closed thermodynamic cycle. Thus α value is constrained by drug and Tpx2 dose response. The global fitting analysis provided well-constrained values for dissociation constants which were used to determine α values.

References:

1. Marumoto, T., Zhang, D. & Saya, H. Aurora-A - A guardian of poles. *Nat. Rev. Cancer* **5**, 42–50 (2005).
2. Carmena, M. & Earnshaw, W. C. The cellular geography of Aurora kinases. *Nat. Rev. Mol. Cell Biol.* **4**, 842–854 (2003).
3. Joukov, V. & De Nicolo, A. Aurora-PLK1 cascades as key signaling modules in the regulation of mitosis. *Sci. Signal.* **11**, 1–26 (2018).
4. Reboutier, D. *et al.* Aurora a is involved in central spindle assembly through phosphorylation of ser 19 in P150Glued. *J. Cell Biol.* **201**, 65–79 (2013).
5. Ruchaud, S., Carmena, M. & Earnshaw, W. C. Chromosomal passengers: Conducting cell division. *Nat. Rev. Mol. Cell Biol.* **8**, 798–812 (2007).
6. Carmena, M., Wheelock, M., Funabiki, H. & Earnshaw, W. C. The chromosomal passenger complex (CPC): From easy rider to the godfather of mitosis. *Nat. Rev. Mol. Cell Biol.* **13**, 789–803 (2012).
7. Haworth C, Johnson T, Mortlock A, Keen N, T. S. Aurora B couples chromosome alignment with anaphase by targeting BubR1, Mad2, and Cenp-E to kinetochores. *J Cell Biol* **161**, 267–280 (2003).
8. Quartuccio, S. M. & Schindler, K. Functions of Aurora kinase C in meiosis and cancer. *Front. Cell Dev. Biol.* **3**, (2015).
9. Vader, G. & Lens, S. M. A. The Aurora kinase family in cell division and cancer. *Biochim. Biophys. Acta - Rev. Cancer* **1786**, 60–72 (2008).
10. Anand, S., Penrhyn-Lowe, S. & Venkitaraman, A. R. AURORA-A amplification overrides the mitotic spindle assembly checkpoint, inducing resistance to Taxol. *Cancer Cell* **3**, 51–62 (2003).
11. Otto, T. *et al.* Stabilization of N-Myc Is a Critical Function of Aurora A in Human Neuroblastoma. *Cancer Cell* **15**, 67–78 (2009).
12. Jiang, J. *et al.* Direct Phosphorylation and Stabilization of MYC by Aurora B Kinase Promote T-cell Leukemogenesis. *Cancer Cell* **37**, 200-215.e5 (2020).
13. Cheung, C.H.A., Coumar, M.S., Hsieh, H.-P., Chang, J.-Y. Aurora kinase inhibitors in preclinical and clinical testing. *Expert. Opin. Investig. Drugs* **18**,

379–398 (2009).

14. Tong, M. & Seeliger, M. A. Targeting conformational plasticity of protein kinases. *ACS Chem. Biol.* **10**, 190–200 (2015).
15. Bavetsias, V. & Linardopoulos, S. Aurora Kinase Inhibitors: Current Status and Outlook. *Front. Oncol.* **5**, 1–10 (2015).
16. Kollareddy, M. *et al.* Aurora kinase inhibitors: Progress towards the clinic. *Invest. New Drugs* **30**, 2411–2432 (2012).
17. Huse, M. & Kuriyan, J. The conformational plasticity of protein kinases. *Cell* **109**, 275–82 (2002).
18. Levinson, N. M. The multifaceted allosteric regulation of Aurora kinase A. *Biochem. J.* **475**, 2025–2042 (2018).
19. Young, M. A. *et al.* Structure of the kinase domain of an imatinib-resistant Abl mutant in complex with the aurora kinase inhibitor VX-680. *Cancer Res.* **66**, 1007–1014 (2006).
20. Sessa, F. *et al.* Mechanism of Aurora B activation by INCENP and inhibition by hesperadin. *Mol. Cell* **18**, 379–391 (2005).
21. Dubois, N. *et al.* Dynamic architechture of a protein kinase. *Proc. Natl. Acad. Sci.* **111**, 16973–16973 (2014).
22. Kornev, A. P., Haste, N. M., Taylor, S. S. & Ten Eyck, L. F. Surface comparison of active and inactive protein kinases identifies a conserved activation mechanism. *Proc. Natl. Acad. Sci. U. S. A.* **103**, 17783–17788 (2006).
23. Cyphers, S., Ruff, E. F., Behr, J. M., Chodera, J. D. & Levinson, N. M. A water-mediated allosteric network governs activation of Aurora kinase A. *Nat. Chem. Biol.* **13**, 402–408 (2017).
24. Dubois, N. *et al.* Dynamic architecture of a protein kinase Christopher. *Proc. Natl. Acad. Sci.* **111**, 16973–16973 (2014).
25. Ruff, E. F. *et al.* A dynamic mechanism for allosteric activation of Aurora kinase A by activation loop phosphorylation. *Elife* **7**, 1–22 (2018).
26. Lake, E. W. *et al.* Quantitative conformational profiling of kinase inhibitors reveals origins of selectivity for Aurora kinase activation states. *Proc. Natl.*

Acad. Sci. **115**, E11894–E11903 (2018).

27. Hammond, D. *et al.* Melanoma-associated mutations in protein phosphatase 6 cause chromosome instability and DNA damage owing to dysregulated Aurora-A. *J. Cell Sci.* **126**, 3429–3440 (2013).
28. Borisa, A. C. & Bhatt, H. G. A comprehensive review on Aurora kinase: Small molecule inhibitors and clinical trial studies. *Eur. J. Med. Chem.* **140**, 1–19 (2017).
29. D'Alise, A. M. *et al.* Reversine, a novel Aurora kinases inhibitor, inhibits colony formation of human acute myeloid leukemia cells. *Mol. Cancer Ther.* **7**, 1140–1149 (2008).
30. Early, T. R. *et al.* Fragment-Based Discovery of the Pyrazol-4-yl Urea (AT9283), a Multitargeted Kinase Inhibitor with Potent Aurora Kinase Activity † . *J. Med. Chem.* **52**, 379–388 (2008).
31. Pitsawong, W. *et al.* Dynamics of human protein kinase Aurora A linked to drug selectivity. *Elife* **7**, 1–30 (2018).
32. de Groot, C. O. *et al.* A cell biologist's field guide to aurora kinase inhibitors. *Front. Oncol.* **5**, 1–26 (2015).
33. Li, S. *et al.* Spatial compartmentalization specializes the function of Aurora A and Aurora B. *J. Biol. Chem.* **290**, 17546–17558 (2015).
34. Janeček, M. *et al.* Allosteric modulation of AURKA kinase activity by a small-molecule inhibitor of its protein-protein interaction with TPX2. *Sci. Rep.* **6**, 1–12 (2016).
35. Bayliss, R. *et al.* Determinants for Aurora-A activation and Aurora-B discrimination by TPX2. *Cell Cycle* **3**, 402–405 (2004).
36. Fu, J., Bian, M., Liu, J., Jiang, Q. & Zhang, C. A single amino acid change converts Aurora-A into Aurora-B-like kinase in terms of partner specificity and cellular function. *Proc. Natl. Acad. Sci.* **106**, 6939–6944 (2009).
37. Richards, M. W. *et al.* Structural basis of N-Myc binding by Aurora-A and its destabilization by kinase inhibitors. *Proc. Natl. Acad. Sci.* **113**, 13726–13731 (2016).
38. Bhullar, K. S. *et al.* Kinase-targeted cancer therapies: Progress, challenges

and future directions. *Mol. Cancer* **17**, 1–20 (2018).

39. Schaaf, T. M., Peterson, K. C., Grant, B. D., Thomas, D. D. & Gillispie, G. D. Spectral unmixing plate reader: High-throughput, high-precision FRET Assays in living cells. *SLAS Discov.* **22**, 250–261 (2017).
40. Oslob, J. D. *et al.* Discovery of a potent and selective Aurora kinase inhibitor. *Bioorganic Med. Chem. Lett.* **18**, 4880–4884 (2008).
41. Bayliss, C. A. D. ; M. K. ; M. W. R. ; B. A. ; V. B. ; J. B. ; R. Crystal structure of an Aurora-A mutant that mimics Aurora-B bound to MLN8054: insights into selectivity and drug design. *Biochem J* **427**, 19–28
42. Vader, G., Medema, R. H. & Lens, S. M. A. The chromosomal passenger complex: Guiding Aurora-B through mitosis. *J. Cell Biol.* **173**, 833–837 (2006).
43. Carmena, M., Ruchaud, S. & Earnshaw, W. C. Making the Auroras glow: regulation of Aurora A and B kinase function by interacting proteins. *Curr. Opin. Cell Biol.* **21**, 796–805 (2009).
44. Petsalaki, E., Akoumianaki, T., Black, E. J., Gillespie, D. A. F. & Zachos, G. Phosphorylation at serine 331 is required for Aurora B activation. *J. Cell Biol.* **195**, 449–466 (2011).
45. Sessa, F. & Villa, F. Structure of Aurora B-INCENP in complex with barasertib reveals a potential transinhibitory mechanism. *Acta Crystallogr. Sect. FStructural Biol. Commun.* **70**, 294–298 (2014).
46. Bayliss, R., Sardon, T., Vernos, I. & Conti, E. Structural basis of Aurora-A activation by TPX2 at the mitotic spindle. *Mol. Cell* **12**, 851–862 (2003).
47. Abdul Azeez, K. R. *et al.* Structural mechanism of synergistic activation of Aurora kinase B/C by phosphorylated INCENP. *Nat. Commun.* **10**, (2019).
48. Sessa, F. & Villa, F. Structural and Biochemical Analysis of an Aurora B Kinase Mutant Reveals a Multistep Activation Mechanism. *http//www.rcsb.org/structure/4B8M (to be Publ.*